ARTICLE

Quercetin prevents bone loss in hindlimb suspension mice via stanniocalcin 1-mediated inhibition of osteoclastogenesis

Yin-bo Niu[1], Yuan-yuan Yang[1], Xuan Xiao[1,2], Yang Sun[3], Yu-mei Zhou[3], Yu-han Zhang[1], Dong Dong[1], Chen-rui Li[1], Xiang-long Wu[1], Yu-hua Li[4] and Qi-bing Mei[1,4]

Recent studies demonstrate that diet quercetin (Quer) has obvious bone protective effects on ovariectomized rodents but thus far there is no direct evidence to support the inhibitory effect of Quer on bone loss caused by long-term unloading. In the present study, we investigated whether Quer could prevent bone loss induced by unloading in mice. Mice were subjected to hindlimb suspension (HLS) and received Quer (25, 50, 100 mg·kg^{-1}·day^{-1}, ig) for 4 weeks. Before euthanasia blood sample was collected; the femurs were harvested and subjected to MicroCT analysis. We showed that Quer administration markedly improved bone microstructure evidenced by dose-dependently reversing the reduction in bone volume per tissue volume, trabecular number, and bone mineral density, and the increase of trabecular spacing in mice with HLS. Analysis of serum markers and bone histometric parameters confirmed that Quer at both middle and high doses significantly decreased bone resorption-related markers collagen type I and tartrate-resistant acid phosphatase 5b, and increased bone formation-related marker procollagen 1 N-terminal propeptide as compared with HLS group. Treatment with Quer (1, 2, 5 μM) dose-dependently inhibited RANKL-induced osteoclastogenesis through promoting the expression of antioxidant hormone stanniocalcin 1 (STC1) and decreasing ROS generation; knockdown of STC1 blocked the inhibitory effect of Quer on ROS generation. Knockdown of STC1 also significantly promoted osteoclastogenesis in primary osteoclasts. In conclusion, Quer protects bones and prevents unloading-caused bone loss in mice through STC1-mediated inhibition of osteoclastogenesis. The findings suggest that Quer has the potential to prevent and treat off-load bone loss as an alternative supplement.

Keywords: quercetin; bone loss; osteoclast; STC1; ROS; hindlimb suspension mice

INTRODUCTION

Prolonged disuse or reduced weightbearing can cause significant bone loss. Disuse osteoporosis is a common skeletal disorder in patients subjected to prolonged immobility or bed rest and astronauts who perform long-duration spaceflight missions [1, 2]. Osteoporosis caused by a lack of adequate loading leads to impaired mobility, increased risk of fractures, poor long-term recovery, and poor quality of life [3]. Several therapeutic interventions, such as resistance exercise, pharmacological treatment, and nutritional strategies, have shown good efficacy in recent years [4–6]. Several prescription drugs, including bisphosphonates and parathyroid hormone, have significant protective effects on bone loss. However, potential adverse side effects such as atrial fibrillation, upper gastrointestinal intolerance, headache, and nausea and the substantial cost of such drugs limit their long-term application [7–10]. The pathology of bone loss remains a key concern, and the exploitation of applicable drugs for the prevention of progressive osteopenia is of urgent importance.

Natural products are excellent and reliable resources for the prevention of bone loss since they have fewer side effects and are more suitable for long-term application compared with chemosynthetic medicines [11, 12]. Flavonoids are natural polyphenols with an extensive distribution in plants, and they are ubiquitous in our daily diet. Quercetin (Quer: 3,5,7,3′,4′-pentahydroxy flavone; molecular weight 302.24 Da) (Fig. 1), a major dietary flavonoid in onion and other vegetables, has attracted great attention for its wide spectrum of biological and pharmacological activities, most of which are related to its antioxidant, anticancer, anti-inflammatory, antimicrobial, antianaphylaxis, and blood lipid-decreasing properties [13–16]. Currently, there is growing concern regarding the treatment of osteoporosis based on the beneficial effects of chemoprophylaxis and the therapeutic action of Quer [17]. Recent studies have confirmed that dietary Quer could increase bone density and alter bone histomorphology in ovariectomized mice and rats [18–20]. However, there has been no direct evidence of the protective effects of Quer on bone loss induced by prolonged disuse or lightened loading until now. In addition, little is known about the mechanisms of the effects of Quer on disuse osteoporosis. Therefore, our study aims to evaluate the function and mechanism of Quer in bone metabolism in hindlimb

[1]Key Laboratory for Space Bioscience and Biotechnology, School of Life Sciences, Northwestern Polytechnical University, Xi'an 710072, China; [2]Department of Cell Biology and Genetics, School of Basic Medical Sciences, Xi'an Jiaotong University Health Science Center, Xi'an 710061, China; [3]Key Laboratory of Gastrointestinal Pharmacology of Chinese Materia Medica of the State Administration of Traditional Chinese Medicine, Department of Pharmacology, School of Pharmacy, The Fourth Military Medical University, Xi'an 710032, China and [4]Department of Pharmacology, School of Pharmacy, Southwest Medical University, Luzhou 646000, China
Correspondence: Yu-hua Li (yuhualee973@aliyun.com) or Qi-bing Mei (qbmei@fmmu.edu.cn)

Quer prevents hindlimbs suspension-caused bone loss
YB Niu et al.

1477
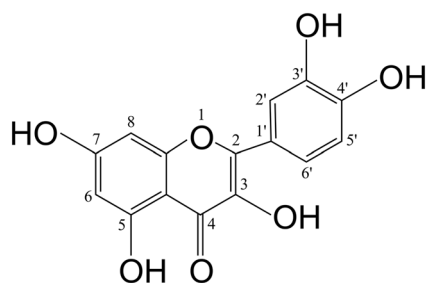
Fig. 1   Quer, 3,5,7,3′,4′-pentahydroxy flavone used in this study. Chemical structures of Quer.

suspension (HLS) mice (a model that has been extensively used for simulating unloading associated with spaceflight microgravity, muscle atrophy, and disuse osteopenia) [2, 21].

MATERIALS AND METHODS

Reagents and antibodies
Quer (purity > 99%, HPLC) was purchased from the National Institutes for Food and Drug Control (Beijing, China). Raw264.7 macrophages were obtained from the Shanghai Cell Bank of the Chinese Academy of Sciences. Alpha-minimal essential medium (α-MEM) and the penicillin/streptomycin antibiotic mixture were purchased from HyClone Laboratories, Inc. (Logan, UT, USA). Fetal bovine serum was purchased from BI (Kibbutz Beit-Haemek, Israel). Recombinant murine RANKL (sRANKL) was purchased from Pepro Tech EC Co., Ltd. (Rocky Hill, NJ, USA). *Escherichia coli* lipopolysaccharide (LPS), calcein, and naphthol AS-MS phosphate were purchased from Sigma-Aldrich, Inc. (Sigma-Aldrich Corp., St Louis, USA). Cell counting kit 8 and a tartrate-resistant acid phosphatase (TRAP) staining kit were purchased from Dojindo (Tokyo, Japan) and Nanjing Jiancheng Bioengineering Institute (Nanjing, China), respectively. C-terminal crosslinked telopeptides of collagen type I (CTX1), tartrate-resistant acid phosphatase 5b (TRACP5b), and procollagen 1 N-terminal propeptide (P1NP) mouse ELISA kits were purchased from Immunodiagnostic Systems (Fountain Hills, AZ, USA). Tumor necrosis factor alpha (TNF-α) and interleukin-6 (IL-6) were purchased from Cusabio (Wuhan, China). siRNA for stanniocalcin 1 (STC1) (sc-44871) and the negative control (CON) siRNA (sc-37007) were purchased from Santa Cruz Biotechnology (Santa Cruz, CA, USA) and are denoted as Con siRNA and STC1 siRNA, respectively. Mouse anti-STC1 and anti-GAPDH were purchased from HuaBio Inc. (Cambridge, MA, USA) and Bioworld Technology, Inc. (Bloomington, MN, USA), respectively. Mouse anti-JNK, anti-p-JNK, anti-NF-κB, and anti-p-NF-κB antibodies were purchased from Affinity Biosciences LTD (Affinity, Changzhou, China).

Animals and treatments
Thirty 8-week-old WT male C57BL/6J mice (Laboratory Animal Center, Air Force Medical University, Xi-an, China) were used in the study. The mice were fed standard rodent food containing 0.9% calcium and 0.7% phosphate ad libitum (Animal Center of the Key Laboratory of Space Bioscience and Biotechnology, Xi-an, China). After 7 days of acclimatization, the mice were divided into five groups with six mice in each group: ground CON group, HLS group, HLS treatment group with HLS + Quer-L, 25 mg·kg^{-1}·day^{-1}, HLS treatment group with HLS + Quer-M, 50 mg·kg^{-1}·day^{-1}, and HLS treatment group with HLS + Quer-H, 100 mg·kg^{-1}·day^{-1}. The mice in the CON group were allowed to move freely without HLS, but the tails of mice in the other groups were suspended to unload their hindlimbs according to the recommendations of Morey-Holton and Globus [21]. Quer was administered by intragastric gavage once a day for 4 weeks. The mice in the CON and HLS groups received an equal volume of distilled water vehicle for

4 weeks and were injected with 15 mg/kg calcein subcutaneously on days 10 and 3 before necropsy. All mice were handled in accordance with the Guidelines for the Care and Use of Laboratory Animals with the approval of the Institutional Ethics Committee of Northwestern Polytechnical University.

Serum analysis
The mice were fasted for 4 h, and then their blood was collected from the cheeks before euthanasia. Serum was obtained by centrifuging the blood at $1000 \times g$ for 10 min. The concentrations of CTX1, TRACP5b, and P1NP in serum were measured using mouse ELISA kits. All testing procedures were carried out in accordance with the manufacturer's instructions.

MicroCT analysis
The femurs of the mice were harvested, cleaned, and fixed in 70% ethanol at 4 °C for 7 days. MicroCT analysis was performed using a desktop eXplore Locus SP Pre-Clinical Specimen microCT (GE Healthcare, Madison, WI, USA) according to the recommended guidelines [22]. Briefly, three-dimensional (3D) imaging data were obtained with a voxel size of 12 µm in all spatial directions using the microCT Evaluation Program (V5.0A). Trabecular bone was separated from cortical bone by free drawing regions of interests with the Micro-View program (GE healthcare, Madison, WI, USA) and a multiple Intel® processor-based microCT workstation provided with the scanner. The trabecular bone with a thickness of 1 mm in the growth plate was selected as the region of interest for data analysis. The 3D parameters of the trabecular bone analysis were the bone volume per tissue volume (BV/TV; %), trabecular number (Tb.N; 1/mm), trabecular spacing (Tb.Sp; mm), trabecular thickness (Tb.Th; mm), structural model index (SMI), and bone mineral density (BMD; mg/cc).

The cortical bone with a 0.5 mm thickness 3 mm below the femoral growth plate was selected as the area of interest. The 3D parameters of the cortical bone were the total volume (mm^3), cortical volume (mm^3), and cortical thickness (mm).

Biomechanical testing
Three-point bending experiments were performed using MTS MiniBionix 858 test equipment (MTS Systems, Eden Prairie, MN, USA) to investigate the effect of Quer on bone biomechanics. Both the internal and external dimensions (i.e., width and height) at the support point of the femur were measured. Each specimen was placed on two supports spaced 7 mm apart. A load was applied to the midpoint of the bone at a deformation rate of 2 mm/min until the occurrence of fracture. All the force and displacement data were collected to calculate the biomechanical parameters based on the formulas described previously [23, 24]. The following were the obtained parameters: maximum stress (MPa), Young's modulus (MPa), maximum load (N), stiffness (N/mm), and energy (J).

Dynamic bone histomorphometry
The tibiae were collected and fixed in 4% paraformaldehyde overnight, decalcified in 10% EDTA for 14 d, dehydrated in 95% and 100% xylene, and then embedded in methyl methacrylate. The embedded block was sectioned at a thickness of 10 µm, and the sections were mounted on a glass slide (Leica Microtome, Wetzlar, Germany). The dynamic parameters that were quantified using ImageJ included the mineral deposition rate (MAR) (micrometers per day), mineralized surface (MS/BS) (percentage) per bone surface, and bone formation rate (BFR/BS) (µm^3/µm^2 per day).

Tartrate-resistant acid phosphatase (TRAP) staining
Pictures of red TRAP-positive osteoclasts in the region of trabecular bones of distal femurs and the cortical bone of diaphyseal femurs were captured using an E-800 microscope

1478

(Nikon, Tokyo, Japan). The endocortical osteoclast activity was evaluated by identifying TRAP-positive (red) and TRAP-negative cells. Quantification of TRAP staining was detected as the osteoclast number/endocortical surface (N.Oc/BS, 1/mm^2) and the osteoblast number/endocortical surface (N.Ob/BS, 1/mm^2). Naphthol AS-MS phosphate was used for TRAP staining of decalcified femurs. The percentage of TRAP-stained matrix relative to the total bone matrix area was determined using the k-means segmentation method in ImageJ [25].

Osteoclast induction and assay
RAW264.7 cells (2.5×10^4 cells/well) were cultured in 12-well plates and treated with RANKL (50 ng/mL) and/or Quer (0, 1, 2, or 5 μM). The TRAP-positive monocytes were identified among the cells 2 days later. Then, osteoclasts were induced to differentiate from the cells after they were cultured for 2 days. Cells were immobilized and stained for TRAP activity in accordance with the manufacturer's procedures (Nanjing Jiancheng Institute of Bioengineering, China). TRAP-positive cells with three or more nuclei in each cell were counted as osteoclasts.

The isolation of bone marrow monocytes and the differentiation of primary osteoclasts
Bone marrow monocytes were isolated from the long bones after HLS of 9-week-old male mice for 14 or 28 days. Marrow plugs were flushed with a 1-mL syringe using ice-cold PBS and were cultured in α-MEM with M-CSF (30 ng/mL) for 3 days. Subsequently, the nonadherent cells were discarded, and the adherent cells were further cultured in the presence of RANKL (50 ng/mL) and/or Quer (5 μM) for another 2 or 4 days before qPCR or Trap staining.

Measurement of IL-6 and TNF-α
RAW264.7 cells (1×10^6 cells/well) were pretreated with RANKL and Quer (5 μM) for 48 h and then stimulated with LPS (1 μg/mL) for 24 h. The concentrations of IL-6 and TNF-α were assayed in the supernatant using ELISA kits according to the manufacturer's instructions.

RNA-seq analysis and data processing
RAW264.7 cells were treated with 50 ng/mL RANKL with/without 5 μM Quer for 2 days. Total RNA was extracted using standard protocols, and high-throughput sequencing was performed with the Annotation platform from NovelBio (Shanghai, China). The DEseq2 algorithm was used for differential expression genes (DEGs) analysis of RNA-seq expression profiles (the absolute value of genes for which $P \leq 0.05$ and the log2 (fold change) ≥ 0.585 was set as the threshold of the DEGs). Then, the enrichment analysis of GO function and KEGG pathways was performed for the DEGs.

siRNA transfection
RAW264.7 cells (5×10^4 cells per well in six-well plates) were cultured and transfected with siRNAs (5 nM final concentration) using a commercial kit (Lipofectamine RNAi-MAX reagent, Invitrogen) according to the manufacturer's protocol. RNA was extracted from the cells 24 h after transfection and assayed for STC1 by qPCR to confirm the knockdown of STC1 expression. The knockdown efficiency of STC1 in RAW264.7 cells was ~90%.

RNA extraction, cDNA synthesis, and qPCR
The transfected RAW264.7 cells were seeded in six-well plates at a density of 5×10^5 cells per well and treated with RANKL (50 ng/mL) and/or Quer (5 μM) for 48 h. qPCR was used to detect the expression of STC1. Primary bone marrow cells were flushed from the long bones of mice in each group and then were stimulated with M-CSF (30 ng/mL) for 3 days to generate the bone marrow mesenchymal stem cells (BMMs). BMMs treated with RANKL (50 ng/mL) were induced to differentiate into TRAP-positive osteoclasts. Total RNA was isolated from osteoclasts induced to differentiate from

Table 1. The PCR primers were designed.

Jun	5′ → 3′ F	AAGATGGAAACGACCTTCTACG
	5′ → 3′ R	CTTAGGGTTACTGTAGCCGTAG
Tsc22d3	5′ → 3′ F	CCCTAGACAACAAGATTGAGCA
	5′ → 3′ R	GAATCTGCTCCTTTAGGACCTC
Vegfa	5′ → 3′ F	TAGAGTACATCTTCAAGCCGTC
	5′ → 3′ R	CTTTCTTTGGTCTGCATTCACA
SOCS3	5′ → 3′ F	GAGAGCGGATTCTACTGGAG
	5′ → 3′ R	AGCTTGAGTACACAGTCGAAG
Itgb3	5′ → 3′ F	CATTGTTGATGCTTACGGGAAA
	5′ → 3′ R	ATTGAAGGACAGTGACAGTTCT
Tgfbr1	5′ → 3′ F	AGCTGGCCTTGGTCCTGTGG
	5′ → 3′ R	TGGTGAATGACAGTGCGGTTATGG
Cd109	5′ → 3′ F	TCTCGTTCTTCCGGCACTACCTC
	5′ → 3′ R	TTCCTGCTTCGGCTTGTAGAATGC
STC1	5′ → 3′ F	GAAGTGGTTCGCTGCCTCAA
	5′ → 3′ R	TGAGTGTCAAATTTAGCAGC
Ctsk	5′ → 3′ F	TTGCATCGATGGACACAGAG
	5′ → 3′ R	TGTATAACGCCACGGCAAAG
NFATc1	5′ → 3′ F	CCGTTGCTTCCAGAAAATAACA
	5′ → 3′ R	TGTGGGATGTGAACTCGGAA
GAPDH	5′ → 3′ F	CCCTTAAGAGGGATGCTGCC
	5′ → 3′ R	TACGGCCAAATCCGTTCACA

RAW264.5 and primary osteoclasts according to the manufacturer's instructions. Total RNA (1 μg) was used to synthesize first-strand cDNA for reverse transcription PCR (Tiangen, Beijing, China). The relative expression of genes was calculated by the $2^{-\Delta\Delta Ct}$ method [26]. The PCR primers were shown in Table 1.

Western blotting analysis
The transfected RAW264.7 cells were seeded in six-well plates at a density of 5×10^5 cells per well and treated with RANKL (50 ng/mL) and/or Quer (5 μM) for 48 h. The protein (20 μg) was subjected to 12% SDS-PAGE and transferred to a nitrocellulose membrane (Pall, NY, USA) using a wet system (Bio-Rad, San Diego, CA, USA). Immunodetection was performed with mouse anti-STC1 (1:1000), anti-JNK (1:1000), anti-p-JNK (1:1000), anti-NF-κB (1:1000), anti-p-NF-κB (1:1000), and anti-GAPDH (1:5000) antibodies. Immunoreactive proteins were detected using an enhanced chemiluminescence Western blotting detection system (Millipore, Billerica, MA, USA).

Flow cytometry analysis of intracellular ROS generation
The transfected RAW264.7 cells were seeded in six-well plates at a density of 5×10^5 cells per well and treated with RANKL (50 ng/mL) and/or Quer (5 μM) for 48 h. A flow cytometer was then used to detect the generation of reactive oxygen species. Cells were incubated with serum-free culture medium containing 10 μM DCFH-DA (Beyotime Biotechnology, Shanghai, China) for 30 min at 37 °C and then washed twice with serum-free culture medium to remove extracellular DCFH-DA prior to the detection of intracellular ROS. The cells were resuspended in PBS and subjected to flow cytometric analysis. The test was performed with a FACS Calibur flow cytometer (BD Biosciences), and the data were analyzed by FlowJo software (Treestar, Ashland, OR, USA).

Statistical analysis
Statistical analyses were carried out using GraphPad Prism 8.0 (GraphPad Software Inc., San Diego, CA, USA). Data are expressed as the mean ± SD. Statistical analysis was performed in all groups by one-way ANOVA. $P < 0.05$ was considered statistically significant.

Quer prevents hindlimbs suspension-caused bone loss
YB Niu et al.

1479
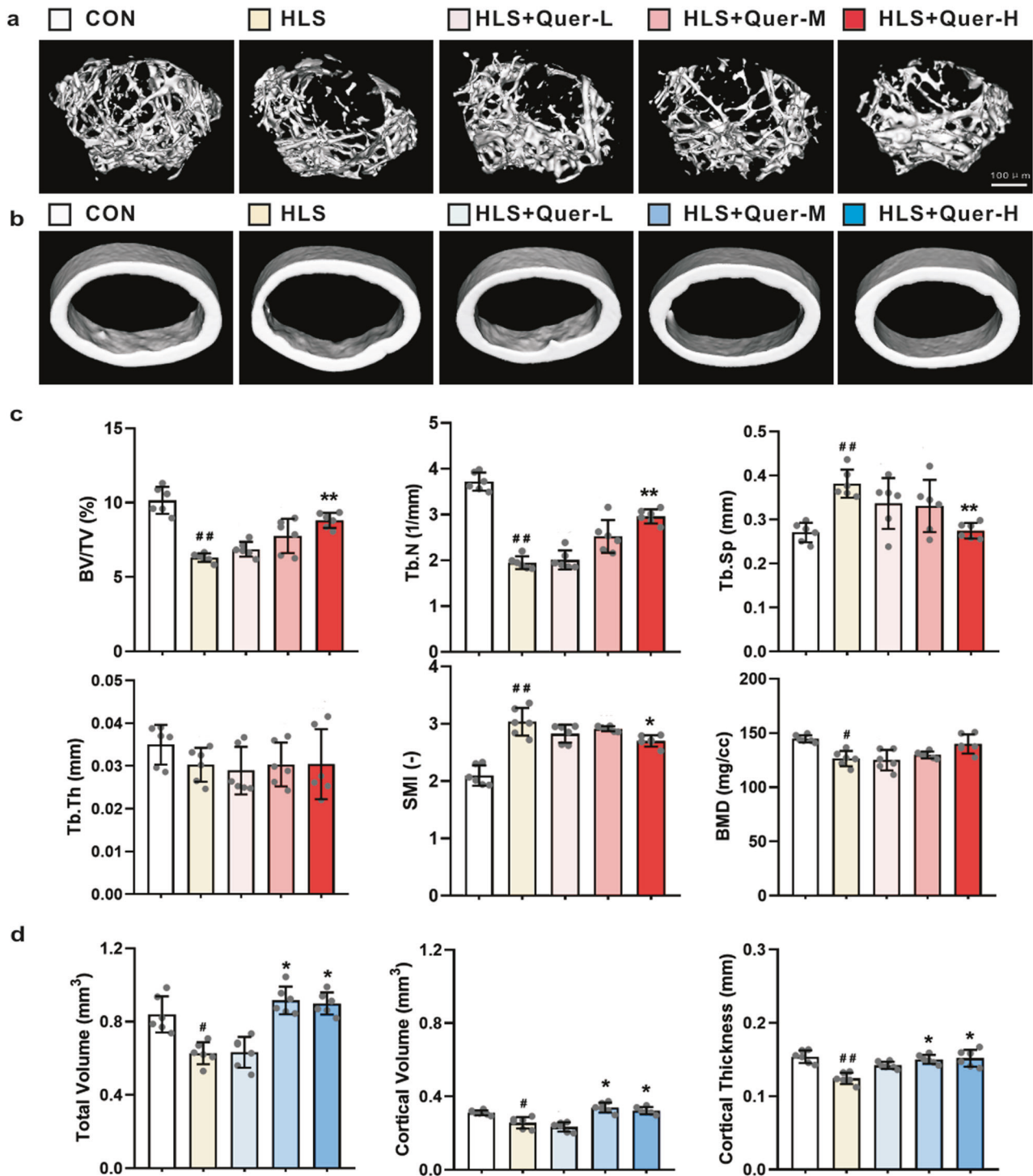
Fig. 2 Quer treatment suppressed bone loss induced by unloading. Representative μCT images of trabecular bones of distal femurs (**a**) and cortical bone of diaphyseal femurs (**b**) from male mice subjected to hindlimb suspension (HLS) for 4 weeks or ground control mice (CON) that were sacrificed at 13 weeks of age. **c** Analysis of the bone volume per tissue volume (BV/TV), trabecular number (Tb.N), trabecular spacing (Tb. Sp), trabecular thickness (Tb.Th), structural model index (SMI), and bone mineral density (BMD) in trabecular bone. **d** Analysis of the total volume, cortical volume, and cortical thickness in cortical bone. The results are represented as the mean ± SD ([#]$P < 0.05$, [##]$P < 0.01$ vs. CON; [*]$P < 0.05$, [**]$P < 0.01$ vs. HLS; $n = 6$ per group).

RESULTS

Quer prevented bone loss and protected the bone microarchitecture from degradation

MicroCT analysis showed that HLS caused severe damage to the cancellous bone and cortical bone of mice. Treatment of HLS mice with high doses of Quer reversed the changes in bone microstructure caused by unloading. Representative pictures of the cancellous bone of mice in each group are shown. Analysis of the cancellous bone characteristics showed that the trabecular BV/TV, Tb.N, and BMD of HLS mice were obviously reduced compared with those of CON mice ($P < 0.05$ or $P < 0.01$). In contrast, the SMI and Tb.Sp of HLS mice were increased compared with those of the

Quer prevents hindlimbs suspension-caused bone loss
YB Niu et al.

1480
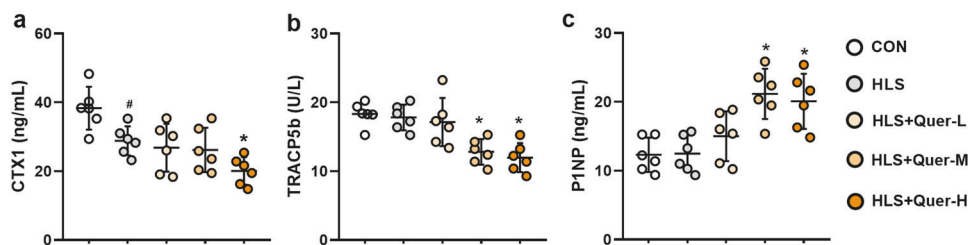
Fig. 3 Effect of Quer treatment on serum chemical markers of bone resorption and bone formation in male mice subjected to hindlimb suspension (HLS) in a 4-week trial that were sacrificed at 13 weeks of age. CON represents the ground control group. **a** CTX1, **b** TRACP5b, and **c** P1NP. The results are represented as the mean ± SD ($^{\#}P < 0.05$ vs. CON; *$P < 0.05$ vs. HLS; $n = 6$ per group).
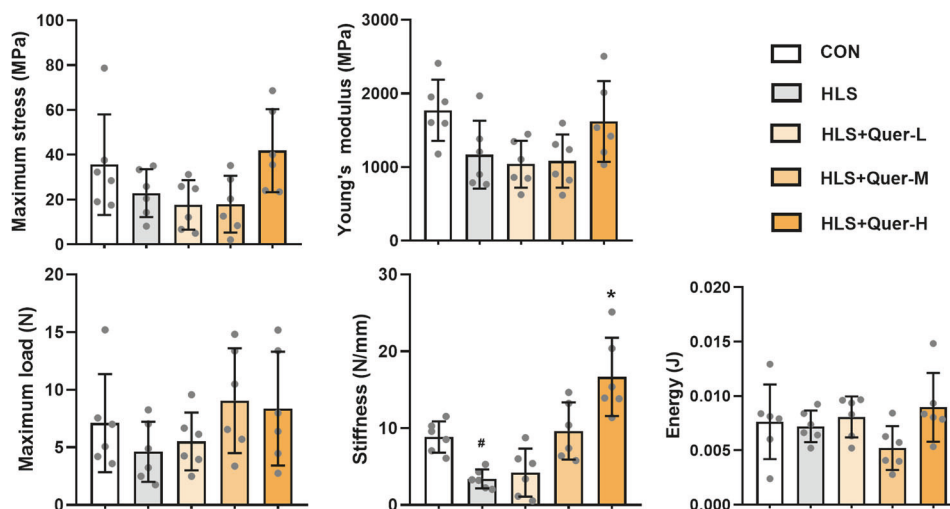
Fig. 4 Effect of Quer treatment on femoral biomechanics as assessed by three-point bending in male mice subjected to hindlimb suspension (HLS) in a 4-week trial that were sacrificed at 13 weeks of age. CON represents the ground control group. Evaluation parameters include the following: maximum stress, Young's modulus, maximum load, stiffness, and energy. The results are represented as the mean ± SD ($^{\#}P < 0.05$ vs. CON; *$P < 0.05$ vs. HLS; $n = 6$ per group).

CON mice ($P < 0.01$). Treatment of HLS mice with Quer reversed the changes in the BV/TV, Tb.N, and Tb.Sp ($P < 0.01$) and protected the microstructure of cancellous bone (Fig. 2c). Representative pictures of the cortical bone of mice in each group are shown in Fig. 2b. Analysis of the cortical bone characteristics in the diaphyseal region showed that HLS caused deterioration of the cortical bone, including a reduction in the total volume, cortical volume, and cortical thickness ($P < 0.05$ or $P < 0.01$). Treatment of HLS mice with 50 and 100 mg·kg^{-1}·day^{-1} Quer reversed the changes caused by unloading ($P < 0.05$) (Fig. 2d).

Effects of Quer on systemic bone turnover markers
CTX1 was reduced by Quer in the HLS group, but the level of TRACP5b remained unchanged compared with that in the CON group ($P < 0.05$). The levels of CTX1 and TRACP5b were further reduced by Quer compared with those in unloaded mice ($P < 0.05$) (Fig. 3a, b). There was no difference in P1NP levels between HLS and CON mice. The level of P1NP was increased by Quer at medium and high doses compared with that in HLS mice ($P < 0.05$) (Fig. 3c).

Effects of Quer on bone biomechanics
The results of the three-point bending experiment showed that there was no significant difference in the femoral biomechanical parameters of each group after hindlimb unloading. However, the maximum stress, Young's modulus, maximum load, and stiffness tended to decrease due to unloading. The high dose of Quer reversed these changes compared with those in unloaded mice ($P < 0.05$) (Fig. 4).

Effects of Quer on bone histomorphology
To determine whether Quer could affect bone surface remodeling and histomorphometry, TRAP staining of osteoclasts in the trabecular bone and cortical bone of the distal femur was performed (Fig. 5a, b). HLS obviously increased the number of TRAP-positive (red signals) cells in the proximal and middle endosteal bone of the femur ($P < 0.01$). Quer at a medium dose and a high dose suppressed the HLS-induced increase in the number of TRAP-positive osteoclasts (osteoclasts/endocortical surface, N.Oc/BS) ($P < 0.05$ or $P < 0.01$), but it had no effect on the number of osteoblasts (osteoblasts/endocortical surface, N.Ob/BS) (Fig. 5c, d). Figure 5e shows a photograph of a tibial specimen with fluorescence double labeling. ImageJ analysis showed that HLS reduced the values of MS/BS, MAR, and BFR/BS ($P < 0.05$). Quer reversed the changes in the values of these parameters caused by unloading ($P < 0.05$ or $P < 0.01$) (Fig. 5f).

Quer suppressed RANKL-induced osteoclastogenesis
The effect of Quer (0, 1, 2, and 5 μM) on RANKL-induced osteoclastogenesis is shown in Fig. 6a. Quer 5 μM had the most obvious inhibitory effect on osteoclastogenesis. Quer remarkably inhibited the formation of TRAP-positive multinucleated cells in a dose-dependent manner ($P < 0.01$) (Fig. 6b).

RNA-seq analysis of RANKL-induced osteoclastogenesis after Quer treatment
RNA-seq of osteoclasts induced to differentiate by RANKL was performed to observe the DEGs related to the inhibition of osteoclast formation by Quer. The Pearson correlation coefficient

Quer prevents hindlimbs suspension-caused bone loss
YB Niu et al.

1481
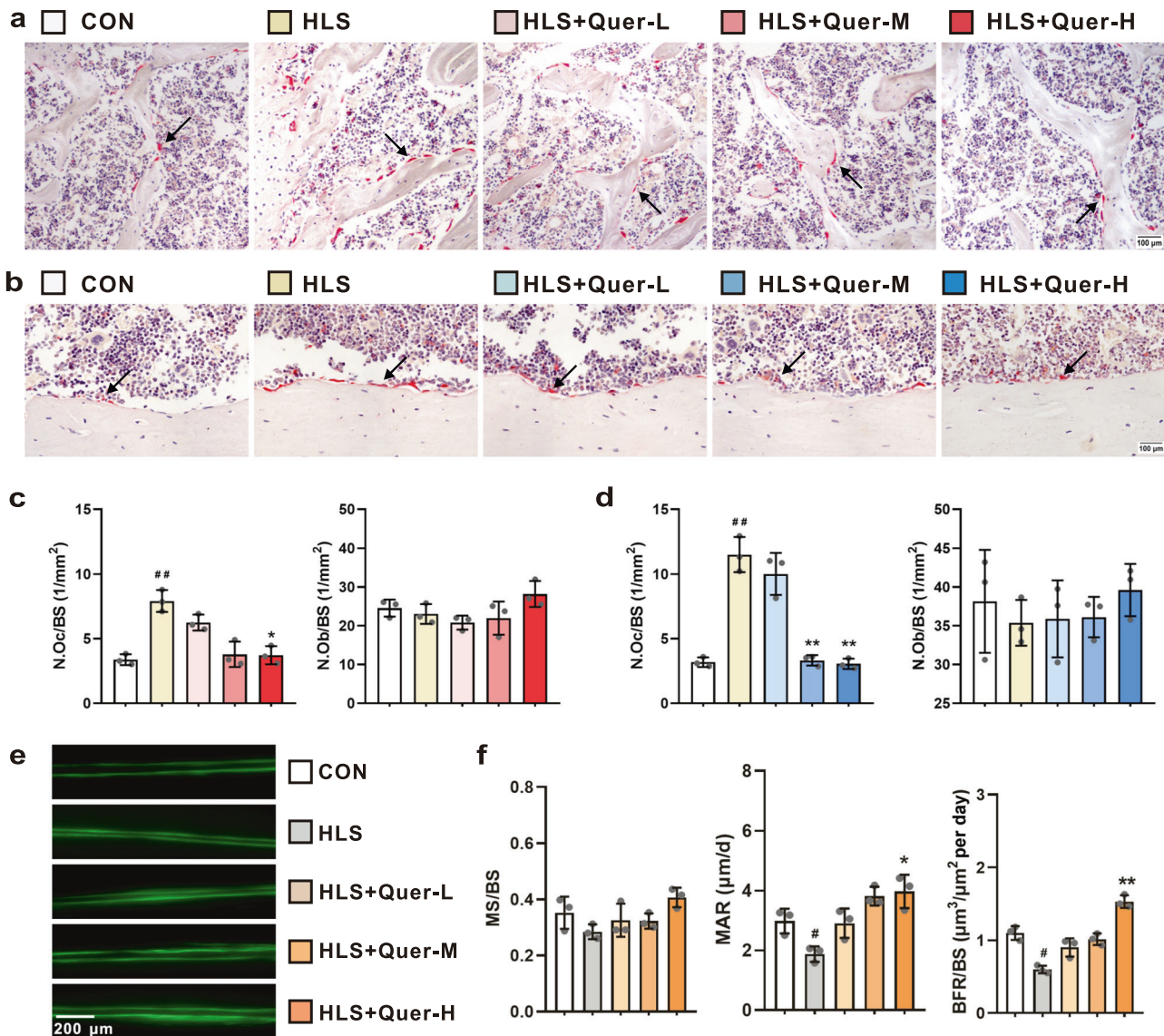
Fig. 5 **Effect of Quer on bone formation and bone resorption as evaluated by bone histomorphometry parameters in male mice subjected to hindlimb suspension (HLS) for 4 weeks that were sacrificed at 13 weeks of age.** CON represents the ground control group. Representative images of TRAP-positive (red) osteoclasts in trabecular bones of distal femurs (**a**) and cortical bone of diaphyseal femurs (**b**). Quantification of TRAP staining in trabecular bones of distal femurs (**c**) and cortical bone of diaphyseal femurs (**d**) according to the osteoclast number/endocortical surface (N.Oc/BS) and osteoblast number/endocortical surface (N.Ob/BS). **e** Mice were injected with 15 mg/kg calcein subcutaneously on days 10 and 3 before necropsy; the embedded tibiae tissue blocks were sectioned at a thickness of 10 μm, and the sections were mounted on a glass slide. **f** Bone histomorphometric analysis revealed the mineralized surface per bone surface (MS/BS), mineral deposition rate (MAR), and bone formation rate (BFR/BS). The results represent the mean ± SD ($^{\#}P < 0.05$, $^{\#\#}P < 0.01$ vs. CON; $^{*}P < 0.05$, $^{**}P < 0.01$ vs. HLS; $n = 3$ per group).

(R^2) reflects the degree of correlation of all samples with an R^2 value > 0.8. The results showed that the R^2 values in both the Con and Quer groups were >0.96 (Supplementary Fig. S1). The DEGs between the Con and 5 μM Quer-treated samples were identified using DESeq. According to the screening criteria of a log2FC > 0.585 or <−0.585 and a FDR<0.05, 1119 differentially expressed genes were identified in osteoclasts of the Con group and Quer treatment group; 439 genes were upregulated, and 680 genes were downregulated (Fig. 6c). Based on the enrichment analysis of GO function and KEGG pathways performed for the DEGs, eight genes related to osteoclast differentiation, osteoclast fusion, bone resorption, and bone development were selected and verified by qPCR (Fig. 6d). Quer upregulated STC1 and SCOCS3 gene expression and reduced Itgb3, Itgbr1, Jun, Vegfa, Tsc22d3, and Cd109 gene expression (P < 0.05 or P < 0.01) (Fig. 6e).

Quer promoted stanniocalcin 1 (STC1) expression and reduced ROS levels in RANKL-induced osteoclasts
qPCR and Western blotting results showed that the effect of Quer on promoting STC1 expression was inhibited by STC1 siRNA (P < 0.05 or P < 0.01) (Fig. 7a–c). The findings of flow cytometry demonstrated that the effect of Quer on reducing ROS levels was blocked by STC1 siRNA (P < 0.05 or P < 0.01) (Fig. 7d, e). The number of osteoclasts was positively correlated with the ROS content (P < 0.05 or P < 0.01) (Fig. 7f, g).

Effects of Quer on IL-6, TNF-α, STC1, JNK, and NF-κB in RANKL-induced osteoclasts
IL-6 and TNF-α expression levels were induced by LPS in the supernatant of RANKL-induced osteoclasts. The levels of IL-6 and TNF-α were reduced by Quer (P < 0.01) (Fig. 6h, i). Quer prevented

Quer prevents hindlimbs suspension-caused bone loss
YB Niu et al.

1482
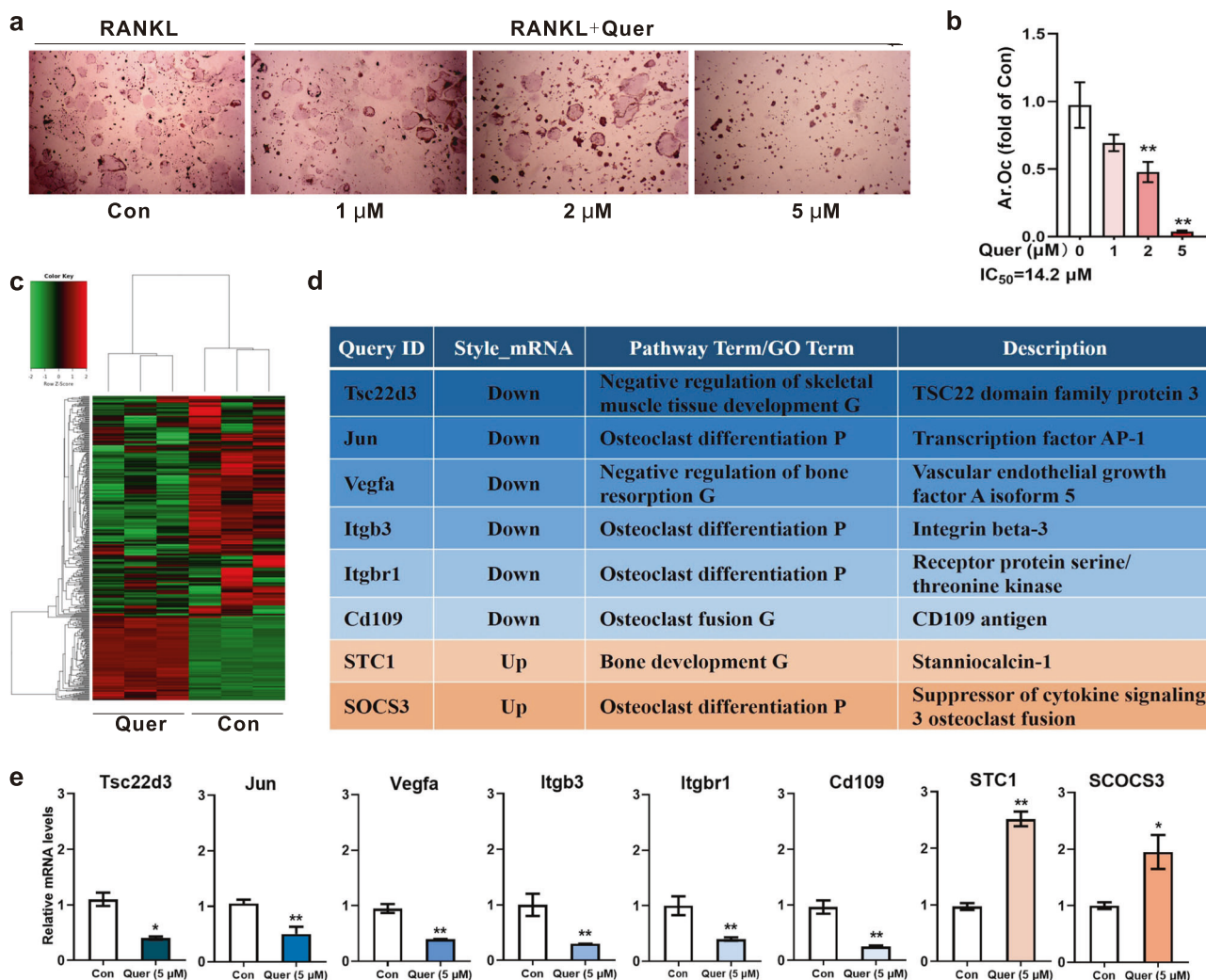
Fig. 6 Quer suppressed RANKL-induced osteoclastogenesis. a Representative images of TRAP-positive osteoclasts. RAW264.7 cells induced by 50 ng/mL RANKL were treated with Quer at concentrations of 1, 2, and 5 μM for 4 days before TRAP staining. **b** The dose-dependent inhibitory effects of Quer on RANKL-induced osteoclastogenesis were evaluated by ImageJ analysis. **c** Cluster analysis of differentially expressed genes was performed with RNA-Seq. RAW264.7 cells induced by 50 ng/mL RANKL were treated with/without 5 μM Quer for 2 days, and the total RNA was extracted and subjected to high-throughput sequencing. **d, e** Based on the enrichment analysis of GO function and KEGG pathways for the DEGs, eight genes related to osteoclast differentiation, osteoclast fusion, bone resorption, and bone development (**d**) were selected and verified by qPCR (**e**). The results are represented as the mean ± SD. *$P < 0.05$, **$P < 0.01$ vs. Con. $n = 3$.

an LPS-induced reduction in STC1 expression (Fig. 6j). In addition, Quer obviously inhibited the expression of p-JNK and p-NF-κB. The reduction of p-JNK and p-NF-κB expression by Quer was blocked by STC1 siRNA (Fig. 6k).

Effects of Quer on STC1, NFATc1, and Ctsk expression and the osteoclastogenesis of osteoclasts ex vivo
We detected the expression of STC1, NFATc1, and Ctsk in osteoclasts induced to differentiate from primary bone marrow cells in each group of mice by qPCR. The results showed that Quer increased the expression of STC1 (Fig. 8a) and inhibited the expression of NFATc1 and Ctsk ($P < 0.05$) (Fig. 8b, c). Primary bone marrow cells were induced to differentiate into TRAP-positive osteoclasts. The TRAP staining results showed that the decrease in osteoclastogenesis induced by Quer was inhibited by STC1 siRNA ($P < 0.05$) (Fig. 8d, e).

DISCUSSION
Prolonged bed rest, disuse, and spaceflight induce disuse bone osteoporosis by damaging the bone microstructure and reducing bone volume. Only 1 month of spaceflight can reduce BMD by ~1.5%, as shown by the substantial bone loss in astronauts [27, 28]. However, the pathology of disuse osteoporosis is still unclear and needs to be clarified for the development of effective countermeasures. A growing number of studies have shown that the intake of flavonoids via the diet is closely related to the reduction of osteoporosis risk [29]. Quer, as a major dietary flavonoid, has aroused our interest for the prevention of osteoporosis. Previous studies on the effects of Quer on osteoporosis in vivo mainly focused on osteoporosis induced by ovariectomy, while our study investigated the pharmacological inhibitory effects and mechanism of Quer in disuse osteoporosis induced by hindlimb unloading in mice.

Our findings showed that Quer at a high dose had obvious bone protective effects. It reduced bone loss in mice subjected to long-term hindlimb unloading by inhibiting bone resorption and effectively increasing bone formation. MicroCT analysis showed that Quer improved the bone microstructure by reversing the decrease in BV/TV and Tb.N in cancellous bone and the increase in Tb.Sp and SMI. Neither unloading nor Quer had an effect on Tb.Th in trabecular bone, the total volume of cortical bone, the cortical

Quer prevents hindlimbs suspension-caused bone loss
YB Niu et al.

1483
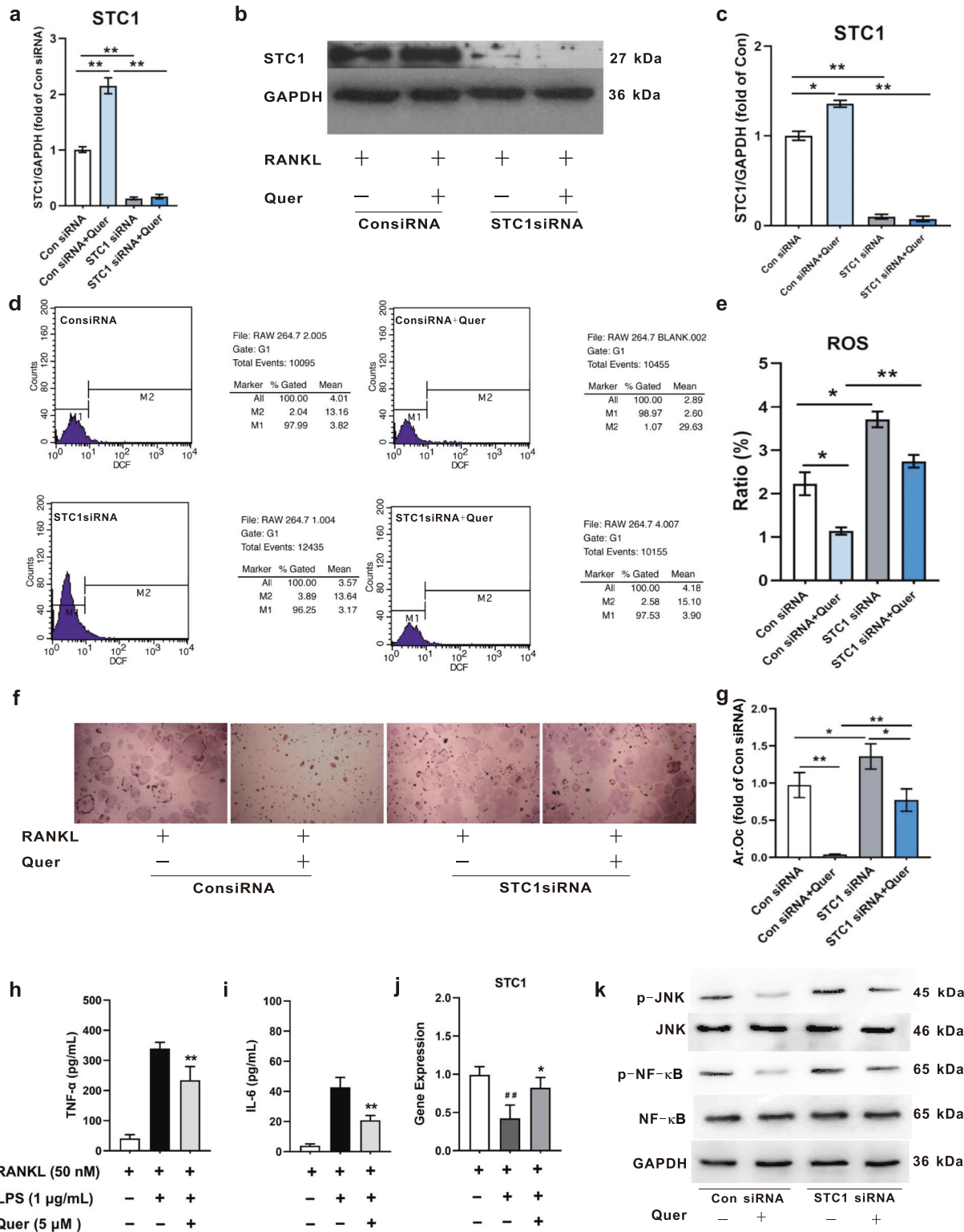
Fig. 7 Quer treatment inhibited RANKL-induced osteoclastogenesis via the STC1-mediated antioxidant pathway. a–e Cells were transfected with STC1 siRNA (STC1 siRNA, 50 nM) or the negative control siRNA (Con siRNA, 50 nM) for 24 h and then treated with RANKL (50 ng/mL) and/or Quer (5 μM) for another 48 h. The effect of Quer on STC1 expression in the Con siRNA and STC1 siRNA groups was measured by qPCR (**a**) and Western blotting (**b**). Densitometric analysis of STC1 is shown in the bar graphs (**c**) (*$P < 0.05$, **$P < 0.01$; $n = 3$). The effect of Quer on ROS production in the Con siRNA and STC1 siRNA groups was measured by flow cytometry (**d**). Quantification of ROS production is shown in the bar graphs (**e**) (*$P < 0.05$, **$P < 0.01$; $n = 3$). **f, g** Cells were transfected with STC1 siRNA (STC1 siRNA, 50 nM) or the negative control siRNA (Con siRNA, 50 nM) for 24 h and then treated with RANKL (50 ng/mL) and/or Quer (5 μM) for another 4 days before TRAP staining (**f**). Quantification of the osteoclast area is shown in the bar graphs (**g**). **h, i** IL-6 and TNF-α expression levels were induced by LPS in the supernatant of RANKL-induced osteoclasts. The levels of IL-6 and TNF-α were reduced by Quer ($P < 0.05$). **j** Quer prevented LPS-induced STC1 reduction. **k** Quer inhibited the expression of p-JNK and p-NF-κB. The effect of Quer on reducing the expression of p-JNK and p-NF-κB was weakened by STC1 siRNA.

Quer prevents hindlimbs suspension-caused bone loss
YB Niu et al.

1484
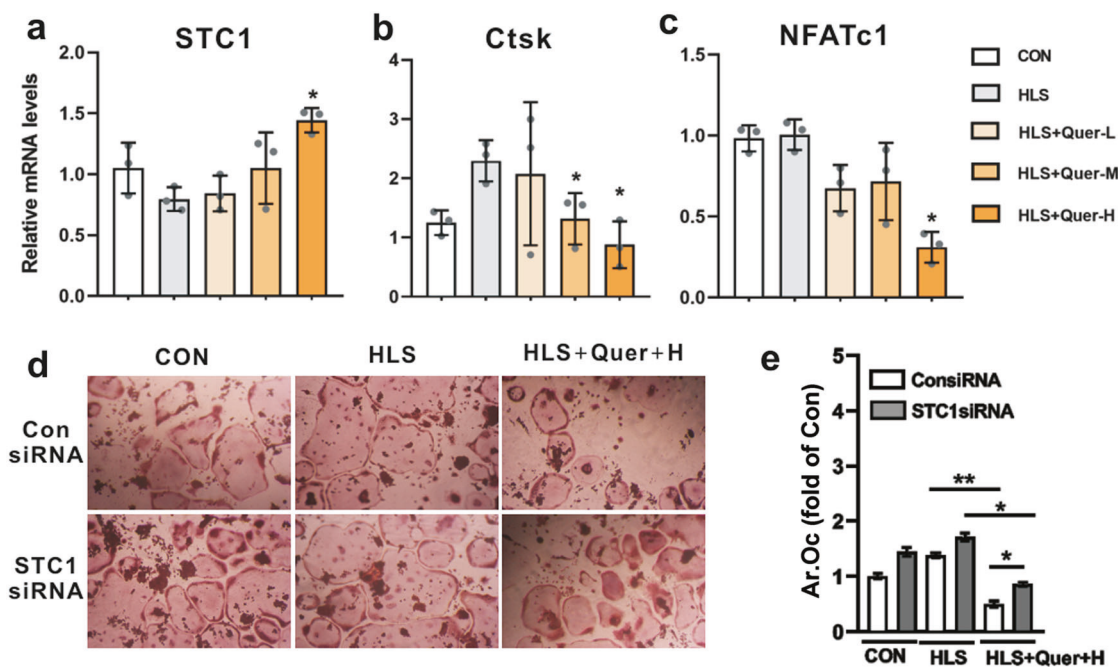
Fig. 8   Effects of Quer on STC1, NFATc1, and Ctsk expression and the osteoclastogenesis of osteoclasts induced to differentiate from primary bone marrow cells. a–c, Quer increased the mRNA expression of STC1 (**a**) and reduced the mRNA expression of Ctsk (**b**) and NFATc1 (**c**) mRNA in primary osteoclasts. The results represent the mean ± SD (*$P < 0.05$ vs. HLS; $n = 3$ per group). **d, e** siSTC1 reduced the inhibitory effect of Quer on osteoclastogenesis in primary osteoclasts (**d**). Quantification of the osteoclast area is shown in the bar graphs (**e**). ($n = 3$ per group).

volume, and the cortical thickness in mice. Among the bone biomechanical parameters in mice, HLS affected only stiffness but had no effect on other indicators, such as maximum stress, Young's modulus, and maximum load and energy, suggesting that Quer can reduce the stiffness of mice in the HLS group. The results of the static index of bone histomorphometry demonstrated that administration of Quer improved the endosteal N.Oc/BS of the trabecular bone and cortical bone of the distal femur in hindlimb unloading mice. Neither hindlimb unloading nor Quer had an effect on the endosteal N.Ob/BS. However, the dynamic index of bone histomorphology showed that Quer at high dose increased MAR and BFR/BS compared with those in the HLS group. Further examination of serum bone turnover markers revealed that the level of CTX1, a marker related to bone resorption, was decreased after hindlimb unloading, but the level of TRACP5b, another marker related to bone resorption, did not change. Quer reduced CTX1 and TRACP5b levels compared with those in the HLS group. The level of P1NP, a marker associated with bone formation, did not change after hindlimb unloading. However, Quer at both the middle and high dose increased the level of P1NP compared with that in the HLS group. All the above results indicate that Quer has the dual effects of promoting bone formation and inhibiting bone resorption, which contributes to resistance to disuse-induced bone loss. At present, studies of the anti-osteoporotic effects and mechanisms of Quer are mainly focused on bone formation. However, our results suggest that Quer has obvious inhibitory effects on osteoclasts. For example, Quer can increase the N.Oc/BS of the trabecular and cortical bone intima of the distal femur in unloaded mice without having an effect on the N.Ob/BS.

In our study, the RNA-Seq transcription analysis of Quer-treated osteoclasts induced by RANKL was performed to reveal the function of Quer in osteoclasts. RNA-seq analysis identified 1119 DEGs in Quer-treated cells, including 439 upregulated genes and 680 downregulated genes. Based on the enrichment analysis of GO function and KEGG pathways for the DEGs, eight genes related to osteoclast differentiation, osteoclast fusion, bone resorption,

and bone development were selected and verified by qPCR. Quer can upregulate STC1 and SCOCS3 gene expression and reduce Itgb3, Jun, Vegfa, Tsc22d3, Itgbr1, and Cd109 gene expression. Previous reports have shown that flavonoids can act as antioxidants to scavenge ROS [13, 30–32]. A growing number of studies have demonstrated that ROS may be the main cause of osteoporosis and that its contribution to oxidative stress plays an important role in osteoporosis [33, 34]. Our findings indicate that Quer can reduce the generation of ROS during RANKL-induced osteoclastogenesis. We found that the antioxidant hormone STC1 was highly expressed in the Quer group based on the gene expression data. STC1, a glycosylated 50-kDa disulfide-linked homodimeric protein, can promote osteoblast development and bone formation as an autocrine/paracrine factor [35]. STC1 is highly expressed in muscle and bone tissue during embryonic development and is mainly associated with osteoblast differentiation and cartilage growth inhibition [36, 37]. This is the first study to show that STC1 can play a role in RANKL-induced osteoclastogenesis. In addition, STC1 was knocked down in RAW264.7 cells using siSTC1 to determine whether Quer could inhibit osteoclastogenesis by regulating STC1 in our study. The results demonstrated that STC1 knockdown can improve ROS production during RANKL-induced osteoclastogenesis. TRAP staining analysis has shown that STC1 knockdown can promote osteoclastogenesis and that the inhibitory effect of Quer on osteoclastogenesis was blocked by siSTC1. In addition, it was confirmed that siSTC1 could reverse the inhibition of osteoclast formation by Quer ex vivo. These findings suggest that STC1 plays an important role in inducing osteoclastogenesis in vitro and in vivo. Furthermore, we found that Quer inhibited the expression of TNF-α and IL-6, which are upstream molecules of STC1, and suppressed the activation of JNK and NF-κB, which are downstream molecules of ROS.

Furthermore, we further observed the expression of STC1, NFATc1, and Ctsk mRNA during osteoclastogenesis by isolating bone marrow cells from the HLS model mice in each group. The findings have shown that Quer can increase the expression of

Quer prevents hindlimbs suspension-caused bone loss
YB Niu et al.

1485

STC1 and inhibit the expression of NFATc1 and Ctsk. NFATc1 integrates RANKL signaling to mediate the terminal differentiation of osteoclasts during HLS, resulting in bone loss in mice [38]. Ctsk is a cysteine protease secreted by osteoclasts and is essential for the degradation of matrix collagen during bone resorption [39]. The decrease in NFATc1 and Ctsk mRNA expression in the Quer group is consistent with the findings of tissue morphology, cell culture, and bone metabolism markers. Taken together, the results indicate that Quer can promote STC1 expression and play a dual role in inhibiting bone resorption.

This study has some limitations. Although Quer can obviously inhibit bone resorption, the molecular mechanism of Quer, the regulation of related proteins, and the role of the target genes identified based on the RNA-seq results require systematic exploration. In addition, our finding that Quer has no effects on a bone formation-related indicator, endocortical N.Ob/BS, but can increase bone formation-related indicators such as serum P1NP and the bone histomorphological indicators MAR and BFR/BS still needs further elucidation. Therefore, we will thoroughly explore the mechanism of Quer involved in promoting bone formation in hindlimb unloading mice in future research. In conclusion, Quer can reduce bone loss induced by unloading in mice and protect bones, which can be achieved by STC1-mediated inhibition of osteoclastogenesis. Our findings suggest that Quer as an alternative supplement can be used to prevent and treat bone loss caused by unloading.

AUTHOR CONTRIBUTIONS
YBN, YHL, and QBM designed the experiments. YBN wrote the paper. YHL, and YMZ, revised the paper. YYY, XX, YS, YHZ, and DD, performed the experiments. YYY, XX, CRL, and XLW, analyzed the data.

ADDITIONAL INFORMATION
The online version of this article (https://doi.org/10.1038/s41401-020-00509-z) contains supplementary material, which is available to authorized users.

Competing interests: The authors declare no competing interests.

REFERENCES
1. Lam H, Qin Y. The effects of frequency-dependent dynamic muscle stimulation on inhibition of trabecular bone loss in a disuse model. Bone. 2008;43:1093–100.
2. DeLong A, Friedman MA, Tucker SM, Krause AR, Kunselman A, Donahue HJ, et al. Protective effects of controlled mechanical loading of bone in C57BL6/J mice subject to disuse. JBMR. 2019;4:e10322.
3. Lloyd SA, Lang CH, Zhang Y, Paul EM, Laufenberg LJ, Lewis GS, et al. Inter-dependence of muscle atrophy and bone loss induced by mechanical unloading. J Bone Miner Res. 2014;29:1118–30.
4. Shackelford LC, LeBlanc AD, Driscoll TB, Evans HJ, Rianon NJ, Smith SM, et al. Resistance exercise as a countermeasure to disuse-induced bone loss. J Appl Physiol. 2004;97:119–29.
5. Elliot-Gibson V, Bogoch ER, Jamal SA, Beaton DE. Practice patterns in the diagnosis and treatment of osteoporosis after a fragility fracture: a systematic review. Osteoporos Int. 2004;15:767–78.
6. Southmayd EA, Hellmers AC, De Souza MJ. Food versus pharmacy: assessment of nutritional and pharmacological strategies to improve bone health in energy-deficient exercising women. Curr Osteoporos Rep. 2017;15:459–72.
7. Leblanc A, Matsumoto T, Jones J, Shapiro J, Lang T, Shackelford L, et al. Bisphosphates as a supplement to exercise to protect bone during long-duration spaceflight. Osteoporos Int. 2013;24:2105–14.
8. Silva BC, Bilezikian JP. Parathyroid hormone: anabolic and catabolic actions on the skeleton. Curr Opin Pharmacol. 2015;22:41–50.
9. Chen JS, Sambrook PN. Antiresorptive therapies for osteoporosis: a clinical overview. Nat Rev Endocrinol. 2011;8:81–91.
10. Haas AV, LeBoff MS. Osteoanabolic agents for osteoporosis. J Endocr Soc. 2018;2:922–32.
11. An J, Yang H, Zhang Q, Liu C, Zhao J, Zhang L, et al. Natural products for treatment of osteoporosis: the effects and mechanisms on promoting osteoblast-mediated bone formation. Life Sci. 2016;147:46–58.
12. Wang T, Liu Q, Tjhioe W, Zhao J, Lu A, Zhang G, et al. Therapeutic potential and outlook of alternative medicine for osteoporosis. Curr Drug Targets. 2017;18:1051–68.
13. Shen F, Zhong H, Ge W, Ren J, Wang X. Quercetin/chitosan-graft-alpha lipoic acid micelles: a versatile antioxidant water dispersion with high stability. Carbohydr Polym. 2020;234:115927.
14. Bischoff SC. Quercetin: potentials in the prevention and therapy of disease. Curr Opin Clin Nutr Metab Care. 2008;11:733–40.
15. Khan F, Niaz K, Maqbool F, Ismail Hassan F, Abdollahi M, Nagulapalli Venkata KC, et al. Molecular targets underlying the anticancer effects of quercetin: an update. Nutrients. 2016;8:E529.
16. Ou QW, Zheng ZF, Zhao YY, Lin WQ. Impact of quercetin on systemic levels of inflammation: a meta-analysis of randomised controlled human trials. Int J Food Sci Nutr. 2020;71:152–63.
17. Ahmad N, Banala VT, Kushwaha P, Karvande A, SharmaS, Tripathi AK, et al. Quercetin-loaded solid lipid nanoparticles improve osteoprotective activity in an ovariectomized rat model: a preventive strategy for post-menopausal osteoporosis. RSC Adv. 2016;6:97613–28.
18. Tsuji M, Yamamoto H, Sato T, Mizuha Y, Kawai Y, Taketani Y, et al. Dietary quercetin inhibits bone loss without effect on the uterus in ovariectomized mice. J Bone Miner Metab. 2009;27:673–81.
19. Zhou YN, Wu YQ, Ma WD, Jiang XQ, Takemra A, Uemura M, et al. The effect of quercetin delivery system on osteogenesis and angiogenesis under osteoporotic conditions. J Mater Chem B. 2017;5:612–25.
20. Yuan Z, Min J, Zhao YW, Cheng QF, Wang K, Lin SJ, et al. Quercetin rescued TNF-alpha-induced impairments in bone marrow-derived mesenchymal stem cell osteogenesis and improved osteoporosis in rats. Am J Transl Res. 2018;10:4313–21.
21. Morey-Holton ER, Globus RK. Hindlimb unloading rodent model: technical aspects. J Appl Physiol. 2002;92:1367–77.
22. Bouxsein ML, Boyd SK, Christiansen BA, Guldberg RE, Jepsen KJ, Müller R. Guidelines for assessment of bone microstructure in rodents using micro-computed tomography. J Bone Miner Res. 2010;25:1468–86.
23. Brodt MD, Ellis CB, Silva MJ. Growing C57Bl/6 mice increase whole bone mechanical properties by increasing geometric and material properties. J Bone Miner Res. 1999;14:2159–66.
24. Turner CH, Burr DB. Basic biomechanical measurements of bone: a tutorial. Bone. 1993;14:595–608.
25. Tang SY, Herber RP, Ho SP, Alliston T. Matrix metalloproteinase-13 is required for osteocytic perilacunar remodeling and maintains bone fracture resistance. J Bone Miner Res. 2012;27:1936–50.
26. Livak KJ, Schmittgen TD. Analysis of relative gene expression data using realtime quantitative PCR and the 2(-Delta Delta C(T)) method. Methods. 2001;25:402–8.
27. Wattel A, Kamel S, Prouillet C, Petit JP, Lorget F, Offord E, et al. Flavonoid quercetin decreases osteoclastic differentiation induced by RANKL via a mechanism involving NF kappa B and AP-1. J Cell Biochem. 2004;92:285–95.
28. Smith SM, Heer MA, Shackelford LC, Sibonga JD, Ploutz-Snyder L, Zwart SR. Benefits for bone from resistance exercise and nutrition in long-duration spaceflight: evidence from biochemistry and densitometry. J Bone Miner Res. 2012;27:1896–906.
29. Chen YM, Ho SC, Lam SS, Ho SS, Woo JL. Soy isoflavones have a favorable effect on bone loss in Chinese postmenopausal women with lower bone mass: a double-blind, randomized, controlled trial. J Clin Endocrinol Metab. 2003;88:4740–7.
30. Agati G, Azzarello E, Pollastri S, Tattini M. Flavonoids as antioxidants in plants: location and functional significance. Plant Sci. 2012;196:67–76.
31. Pandhair V, Sekhon BS. Reactive oxygen species and antioxidants in plants: an overview. J Plant Biochem Biotechnol. 2006;15:71–8.
32. Qureshi MK, Munir S, Shahzad AN, Rasul S, Nouman W, Aslam K. Role of reactive oxygen species and contribution of new players in defense mechanism under drought stress in rice. Int J Agric Biol. 2018;20:1339–52.
33. Bartell SM, Kim HN, Ambrogini E, Han L, Iyer S, Ucer SS, et al. FoxO proteins restrain osteoclastogenesis and bone resorption by attenuating H2O2 accumulation. Nat Commun. 2014;5:3773.

1486

34. AlQranei MS, Aljohani H, Majumdar S, Senbanjo LT, Chellaiah MA. C-phycocyanin attenuates RANKL-induced osteoclastogenesis and bone resorption in vitro through inhibiting ROS levels, NFATc1 and NF-κB activation. Sci Rep. 2020;10:2513.

35. Yoshiko Y, Aubin JE, Maeda N. Stanniocalcin 1 (STC1) protein and mRNA are developmentally regulated during embryonic mouse osteogenesis: the potential of stc1 as an autocrine/paracrine factor for osteoblast development and bone formation. J Histochem Cytochem. 2002;50:483–92.

36. Terra SR, Cardoso JC, Félix RC, Martins LA, Souza DO, Guma FC, et al. STC1 interference on calcitonin family of receptors signaling during osteoblastogenesis via adenylate cyclase inhibition. Mol Cell Endocrinol. 2015;403:78–87.

37. Brum AM, van de Peppel J, Nguyen L, Aliev A, Schreuders-Koedam M, Gajadien T, et al. Using the connectivity map to discover compounds influencing human osteoblast differentiation. J Cell Physiol. 2018;233:4895–906.

38. Takayanagi H, Kim S, Koga T, Nishina H, Isshiki M, Yoshida H, et al. Induction and activation of the transcription factor NFATc1 (NFAT2) integrate RANKL signaling in terminal differentiation of osteoclasts. Dev Cell. 2002;3:889–901.

39. Zenger S, Hollberg K, Ljusberg J, Norgård M, Ek-Rylander B, Kiviranta R, et al. Proteolytic processing and polarized secretion of tartrate-resistant acid phosphatase is altered in a subpopulation of metaphyseal osteoclasts in cathepsin K-deficient mice. Bone. 2007;41:820–32.